CHEMISTRY OF MATERIALS

Article

pubs.acs.org/cm

Highly Versatile Approach for Preparing Functional Hybrid Multisegmented Nanotubes and Nanowires

Cecile J. Roy,[†] Nicolas Chorine,[†] Bruno G. De Geest,[‡] Stefaan De Smedt,[§] Alain M. Jonas,[†] and Sophie Demoustier-Champagne*[,†]

[†]Institute of Condensed Matter and Nanosciences - Bio & Soft Matter (IMCN/BSMA), Université Catholique de Louvain, Croix du Sud 1, L7.04.02, B-1348 Louvain-la-Neuve, Belgium

[‡]Laboratory of Pharmaceutical Technology and [§]Laboratory of General Biochemistry & Physical Pharmacy, Ghent University, Harelbekestraat 72, B-9000 Ghent, Belgium

Supporting Information

ABSTRACT: The membrane-templating method was successfully combined with electrodeposition and layer-by-layer assembly to create various multisegmented nanostructures composed of metal, polymers, synthetic and biological polyelectrolytes, and colloids. The electrochemical approach offers the control over the architectural parameters of the resulting structures (in particular the segment length and morphology), whereas the LbL adsorption technique permits to integrate nonconducting materials, including biomacromolecules, within the nanostructures. A supplementary degree of complexity can be reached by capping or loading the LbL nanotubes with colloidal particles. The ability to easily generate such hybrid anisotropic nanoparticles with spatially resolved chemical, physical, and biochemical functionalities is a boon for the synthesis of nanostructures, which is of tremendous importance for electronic, sensing, drug delivery, and modern biomedical and biotechnological applications.

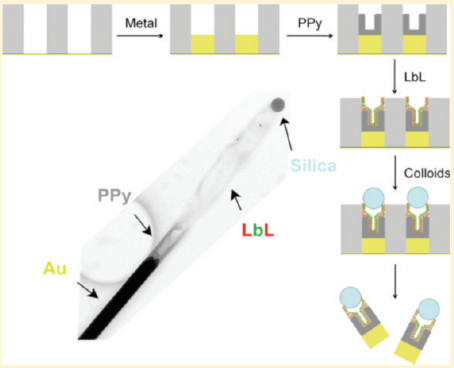

KEYWORDS: *membrane-template, layer-by-layer assembly, electrodeposition, segmented nanostructures, colloids, biomacromolecules, polypyrrole*

INTRODUCTION

Nanorods and nanotubes consisting of segments of different materials that can either perform specific functions or selectively interact with specific ligands have emerged as a new class of advanced one-dimensional (1D) nanomaterials.[1−8] The multisegmented architecture of the nanostructures, along with the ability to vary the block length and the aspect ratio, can indeed lead to nanomaterials presenting a wide range of chemical, physical and biochemical properties that are useful in many applications such as nanoelectronics, (bio)chemical sensing, and drug delivery devices.[4,9−17] The engineering and fabrication of such hybrid nanostructures have therefore received significant attention over the past few years, but there are still relatively few examples of methods for synthesizing multicomponent 1D materials made from both organic and inorganic materials. So far, sequential electrodeposition within the nanopores of a template, either track-etched polycarbonate (PC) or alumina membranes, remains the predominant methods used to synthesize multicomponent nanowires or nanorods.[2−5,15,16,18] On one hand, the membrane provides cylindrical, uniform, well-defined pores, and on the other hand, the electrochemical method provides an excellent control over the architectural parameters (block length and morphology) of the resulting structures but imposes severe limitations on the range of materials that can be processed since only conducting materials (metals, inorganic semiconductors, and conducting polymers) can be deposited.[4,8,19−23] On the other hand, the membrane-templated layer-by-layer adsorption technique, based on the alternate deposition of complementary species such as oppositely charged polyelectrolytes within the pores of a template, has been shown to be an experimentally simple but powerful method to integrate many various functional materials, such as synthetic or biological macromolecules, dyes, and nanoparticles into nanotubes and nanowires.[24−34] In this contribution, we report on a versatile way of synthesizing and assembling hybrid multisegmented functional nanostructures of higher complexity (Scheme 1). The membrane-templated method is combined with electrodeposition and layer-by-layer (LbL) techniques to sequentially synthesize bisegmented and trisegmented nanostructures composed of metals, polymers, synthetic and biological polyelectrolytes and colloids. This new methodology is able to provide multifunctional nanowires and nanotubes of unprecedented complexity and of exquisitely controlled structures that could find applications in fields as diverse as catalysis, electronics, or drug delivery.

Received: November 2, 2011
Revised: April 11, 2012
Published: April 12, 2012

Scheme 1. Membrane-Templated Strategy to Synthesize Bisegmented (M/PPY or M/LbL) and Trisegmented (M/PPy/LbL) Nanostructured Materials

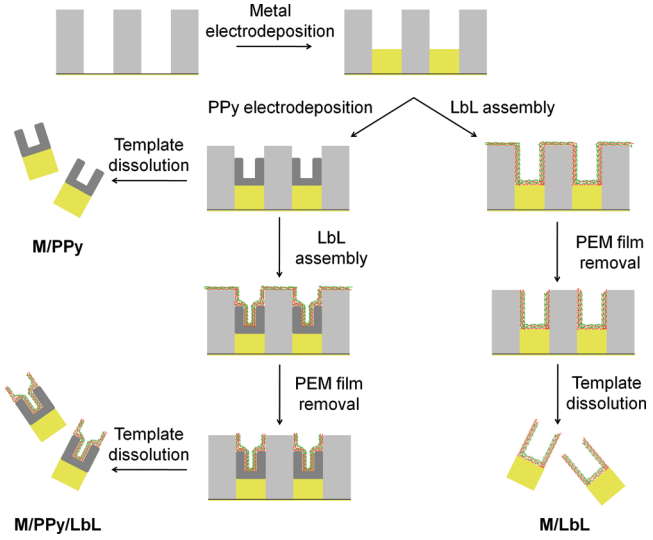

MATERIALS AND METHODS

Materials. Pyrrole (Py), lithium chloride ($LiClO_4$), potassium chloride (KCl), potassium hydrogenophosphate (K_2HPO_4), nickel(II) sulfate hexahydrate ($NiSO_4.6H_2O$), double-stranded DNA sodium salt (DNA of molar mass $M_w \approx 50-100$ kDa) and poly(sodium-p-styrenesulfonate) (PSS of $M_w \approx 70$ kDa) were purchased from Acros. Hydrogen tetrachloroaurate trihydrate ($HAuCl_4.3H_2O$, 99.9%), poly(allylamine hydrochloride) (PAH of $M_w \approx 56$ kDa), and poly(allylamine hydrochloride)-fluorescein isothiocyanate (PAH^{FITC} of $M_w \approx 15$ kDa), with a monomer to dye ratio PAH:FITC equals to 50:1, were purchased from Sigma Aldrich. Boric acid (H_3BO_3) was obtained from UCB. Poly(β-amino ester) (PAE of $M_w \approx 22$ kDa, Scheme 2) was synthesized by Michael addition of bis (secondary amines) to diacrylate esters (4,4′-trimethylenedipiperidine and 1,6-hexanediol diacrylate, respectively) in analogy to methods previously reported.[35,36] Before use, pyrrole monomer was purified by passing it through a micropipet filled with neutral alumina while other products were used as received. The different aqueous solutions were prepared with ultrapure water, with a resistivity of 18.2 mΩ, produced from an Elga system. Track-etched polycarbonate (PC) membranes were provided by *It4ip* (Seneffe, Belgium, www.it4ip.be) with pore diameter ranging from 100 to 200 nm, a thickness of 10 μm, and a density of 1×10^8 pores/cm^2. The cross-section of the template is 1.13 cm^2. Silica nanoparticles and citrate-reduced gold nanoparticles were purchased from Polysciences.

Scheme 2. PAE Synthesis by Michael Addition

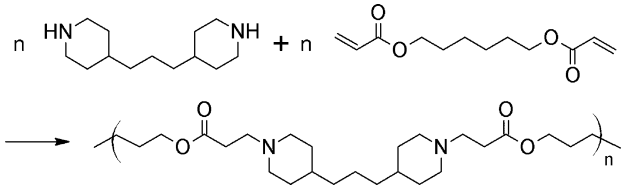

Electrochemical Synthesis of Gold and Polypyrrole Nanostructures. The electrosyntheses were performed with a CHI660B Electrochemical Workstation (CH Inc.) in a one-compartment cell with a Pt counter electrode and a KCl satured Ag/AgCl reference electrode. Nanoporous track-etched polycarbonate membranes were used as templates for the electrochemical growth of the gold (Au), nickel (Ni) and polypyrrole (PPy) segments. To this end, an approximately 450 nm thick layer of Au was evaporated on one side of the PC membrane to serve as the working electrode. Gold or nickel nanowires were first electrodeposited in the pores of the PC membranes. Gold nanowires were synthesized by cycling the potential of the working electrode from 0.7 to 0 V at 200 mV/s using a homemade free-cyanide solution (0.1 M KCl, 0.1 M K_2HPO_4, and 0.03 M $HAuCl_4$ in ultrapure water). Nickel nanowires were electrodeposited by chronoamperommetry at −1.05 V from an aqueous electrochemical bath containing 0.85 M $NiSO_4.6H_2O$ and 0.5 M H_3BO_3. After an abundant rinse with ultrapure water, electrochemical polymerization of pyrrole was carried out by chronoamperommetry at a constant applied potential of 0.75 V. The aqueous monomer solution containing 0.03 M Py monomer and 0.1 M $LiClO_4$ was purged with N_2 for 10 min. The length of each electrosynthesized segment can be controlled by monitoring the charge passed during the electrodeposition process.[3,5,18,21,22]

Layer-by-Layer Assembly. All polyelectrolytes solutions were prepared in 100 mM acetate buffer (pH 4.7) with 0.5 M NaCl at a concentration of 1 mg/mL, except for PAH^{FITC} that was prepared at a concentration of 0.6 mg/mL. In those conditions, $PAH^{(FITC)}$ and PAE, which are weak polycations, are positively charged and may interact with the negatively charged DNA or PSS macromolecules. Besides, this acidic pH permits the aqueous multilayer fabrication with PAE to be carried out without significant polymer degradation on the time scale of the fabrication procedure (e.g., $t_{1/2} \approx 200$ h at pH 5.1, 50 °C).[36,37] All solutions were freshly prepared before use. The PC templates (containing or not the PPy segment) were alternately immersed into the two oppositely charged polyelectrolytes solutions for 30 min each, with two intermediate rinsing steps in the buffer solution for 2 min. This process was repeated until the desired number of bilayers was obtained (a bilayer consists of a polycation layer and a polyanion layer). In presence of PPy segments, the membrane was first exposed to the polyanion bath because of the positively charged surface of the PPy. Otherwise, the LbL deposition started in the polycation bath. This cycled process led to the formation of multilayered nanotubes inside the pores of the template. At the end of LbL assembly, the polyelectrolyte film deposited on the top and the bottom surfaces of the template was removed with a cotton swab immersed in a basic aqueous solution (NaOH, pH 12) 3 M in NaCl and then abundantly rinsed with ultrapure water, as previously reported by Landoulsi et al.[38] The samples were then dried in air overnight.

Colloid Interactions. The nanoparticles were suspended in 100 mM acetate buffer solution at a concentration of 2×10^9 nanoparticles/mL. The nanoparticles buffer solution was chosen so as to avoid premature degradation of the PAE while the nanoparticles concentration was chosen so as to procure ten silica colloids per pore. The nanostructures-containing membranes were exposed to the nanoparticles solution under a slight agitation for 40 h. Before air-drying, the top and bottom surfaces of the membrane were cleaned with cotton swab soaked in ultrapure water in order to remove the nanoparticles interacting with the template surfaces.

Nanostructure Characterization. The nanostructures were observed using a transmission electron microscopy (TEM) and a fluorescent optical microscope. Track-etched polycarbonate membranes were first dissolved by immersion in dichloromethane and the liberated-nanostructures suspension was then dropped and dried on a TEM carbon grid or on a glass microscope slide. The nanostructures were imaged with a LEO922 TEM operating at 200 kV and a LEICA MDR microscope equipped with a FITC filter set and an Epi-Fluorescence module, and connected to a C4742−80−12AG Hamamatsu CDD camera. Fluorescence images were processed using IGOR Pro software (Wavemetrics, Inc.).

RESULTS AND DISCUSSION

Hybrid Bisegmented Nanostructures. Bisegmented nanostructures composed of a metallic nanowire and of an organic LbL nanotube (denoted M/LbL) were constructed in nanopores of a PC template as schematically represented on

dx.doi.org/10.1021/cm203279z | *Chem. Mater.* 2012, 24, 1562−1567

the right side in Scheme 1. The metallic segment (gold or nickel) was first synthesized by electrodeposition at the bottom of the pores and the organic nanotube was then constructed atop by LbL using oppositely charged (bio)polyelectrolytes, namely poly(allylamine hydrochloride) (PAH) or a poly(β-amino ester) (PAE) as polycations and poly(sodium-*p*-styrenesulfonate) (PSS) or double-stranded deoxyribonucleic acid (DNA) as polyanions. Because the surface of the PC membrane bears negative charges, the LbL deposition started with the polycation. After the removal of the multilayer film on the top of the template,[38] the bisegmented M/LbL nanostructures were individually freed from the template by dissolving the membrane and collected for transmission electron microscopy (TEM) characterization. Figure 1 shows

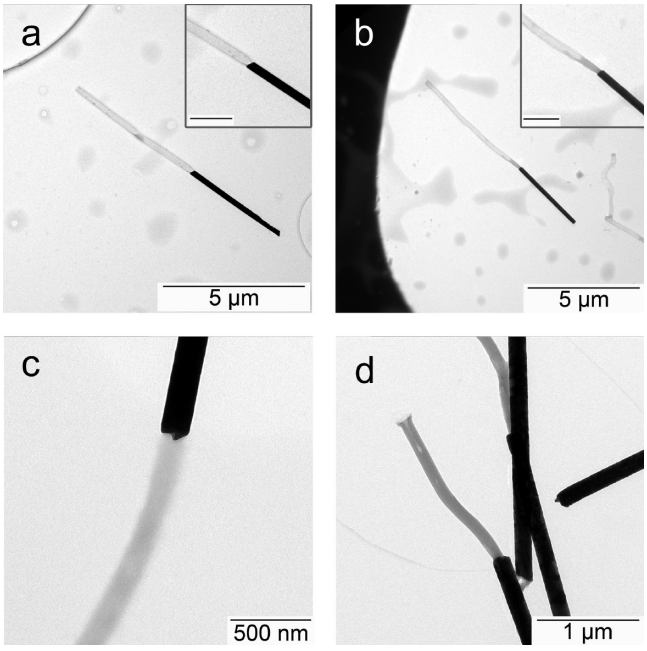

Figure 1. TEM images of bisegmented M/LbL nanostructures composed of a (a, c) gold or (b, d) nickel nanowire, and a (a, b) $(PAH/PSS)_5$ or (c, d) $(PAH/DNA)_5$ LbL segment. The scale bar of the insets is 1 μm.

various bisegmented M/LbL nanostructures composed of a metallic nanowire (Au or Ni) and of a LbL segment (PAH/PSS or PAH/DNA) of 5 bilayers. The polymeric segment appears more transparent than the metallic one because of its lower electronic density. Although the diameter and the total length of the hybrid segmented-nanostructures correspond respectively to the pore diameter and to the thickness of the membrane, the length of the metallic segment can be easily adjusted at the desired length by controlling the amount of charge (related to the number of cycles or to the deposition time) passed during the electrodeposition process (Figure 2). In all cases presented in Figure 1, the LbL segments are observed to be homogeneous along their entire length with a smooth outer surface, indicating that the polyelectrolytes are able to diffuse through the nanopores, allowing the LbL assembly to occur uniformly along the length of the pores walls. The TEM images also show that the PAH/PSS segments exhibit a higher optical density at the edges (Figure 1a, b), typifying a hollow structure (nanotube) while PAH/DNA segments exhibit a more uniform optical density (Figure 1c, d),

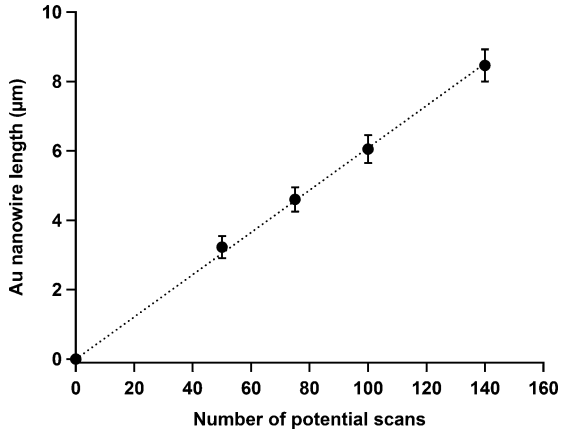

Figure 2. Length of gold nanowires as a function of the number of potential sweeping cycles performed during the electrodeposition.

indicating a filled structure (nanowire). In previous studies, it was reported that the morphology of the LbL segment might be varied from nanotubes to nanowires by tuning the polyelectrolytes, the fabrication conditions (filtration versus immersion, ionic strength of the immersion solutions, molar mass of the polyelectrolytes, pH, etc.), and the number of bilayers.[38] It is also observed that the diameter of the LbL segment constructed atop the Ni segment is significantly smaller than the initial pore diameter. This shrinkage of the LbL segment is due to the multilayer dehydration after the solvent evaporation. Concerning the inorganic−organic interface, it is observed to be relatively flat, indicating that the metallic segments grew homogeneously under our deposition conditions. Despite a small portion of broken nanostructures, the interface can be considered as robust since the interactions taking place between the metallic segment and the LbL segment are strong enough to resist the template dissolution process. Other LbL segments composed of various polyelectrolytes pairs such as PAE/DNA and PAE/PSS were also successfully constructed atop metallic segments in agreement with the previously mentioned general considerations (Figure 3). This demonstrates the ability to

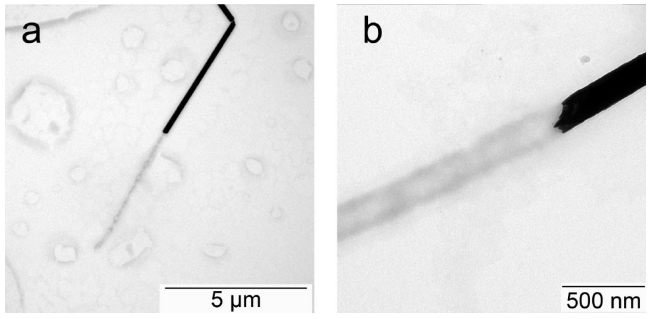

Figure 3. TEM images of bisegmented M/LbL nanostructures composed of (a) a nickel nanowire and a $(PAE/DNA)_5$ LbL segment, and (b) a gold nanowire and a $(PAE/PSS)_5$ LbL segment.

easily synthesize well-defined hybrid bisegmented M/LbL nanostructures composed of various materials through the membrane-templated method.

Trisegmented Nanostructures. By using the membrane-templated strategy schematized on the left side in Scheme 1, a second organic segment, namely a polypyrrole (PPy) segment, was incorporated between the metallic and the LbL segments

dx.doi.org/10.1021/cm203279z | *Chem. Mater.* 2012, 24, 1562–1567

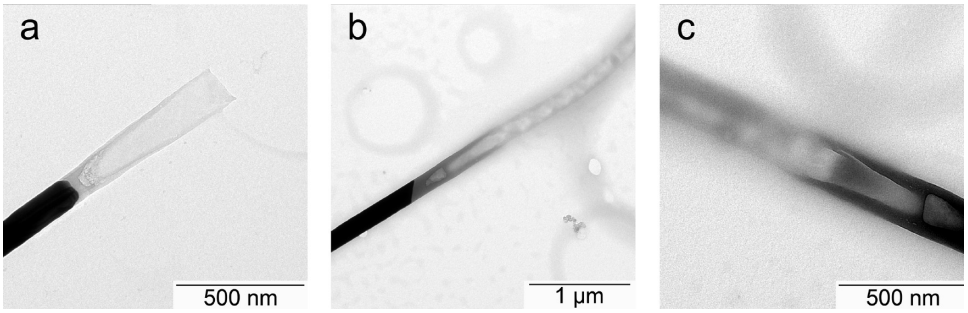

Figure 4. TEM images of (a) a bisegmented M/PPy nanostructure composed of a gold nanowire and a PPy nanotube and (b, c) trisegmented M/PPy/LbL nanostructures composed of a gold nanowire, a PPy nanotube, and a $(DNA/PAH)_5$ LbL nanotube.

to obtain trisegmented nanostructures (denoted M/PPy/LbL). To achieve this, PPy nanotubes were first electrosynthesized atop gold nanowires and then the LbL construction was performed. In order to ensure a good electrostatic interaction between the positively charged PPy segments and the LbL segments, and therefore to obtain a robust PPy/LbL interface, the LbL deposition started with the polyanion. Figure 4 shows TEM images of trisegmented M/PPy/LbL nanostructures composed of an Au nanowire, a PPy nanotube and a $(DNA/PAH)_5$ LbL nanotube. The PPy segments appear in a darker shade of gray atop black gold nanowires and exhibit a tubular morphology of ~1 μm length. As previously reported by our group, the morphology (tube or wire) and the length of the PPy segments can be controlled by the electrosynthesis parameters that are the applied potential and the amount of charges passed during the electropolymerization process, respectively.[18,39] The LbL segments appear in a light shade of gray and extend over the PPy nanotubes for which the cavity exhibits a peculiar blurry aspect (Figure 4c), strongly differing from unfilled PPy nanotubes (Figure 4a).

The use of a polycation labeled with fluorescein (FITC), i.e., PAH^{FITC}, allowed us to investigate the location of the LbL segment in relation to the PPy segment. Figure 5 shows a fluorescent image of the trisegmented M/PPy/LbL nanostructures; the fluorescence profile traced along this nanostructure allows us to identify the three segments: the LbL nanotube exhibits the brightest green emission due to the FITC dyes coupled to the PAH chains, the gold nanowire emits a light green color due to the reflection of the emission light, and the PPy nanotube appears in black in-between. The presence of the LbL segment inside the PPy nanotubes is clearly demonstrated: while an abrupt decrease of the fluorescence intensity is observed at the outer edge of the LbL nanotube, the intensity is progressively decreasing on the side of the PPy segment. The parabolic-shaped curve of the fluorescent intensity in the PPy segment is easily explained by the close-to-quadratic dependence of the amount of fluorescent dyes along the symmetry axis of a cone-shaped PPy segment. The penetration of the LbL segment inside the PPy nanotube increases the surface of adhesion between the PPy and the LbL segments, thereby improving the mechanical strength of this interface as already note for metal/PPy interfaces.[40] It should also be mentioned that the surface treatment performed after the LbL deposition on the top and the bottom surfaces of the template in order to remove the continuous LbL film deposited over these surfaces (soft mechanical polishing with a cotton swab immersed in a basic aqueous solution of high ionic strength), plays a key role in the successful construction of such multisegmented nanostructures. Indeed, without any surface treatment, the observed nanostructures were devoid of the LbL segment because the LbL film deposited onto the membrane surfaces was strongly connected to the LbL segments in the pores, and prevented therefore individualized trisegmented nanostructures from being obtained after the dissolution of the template.

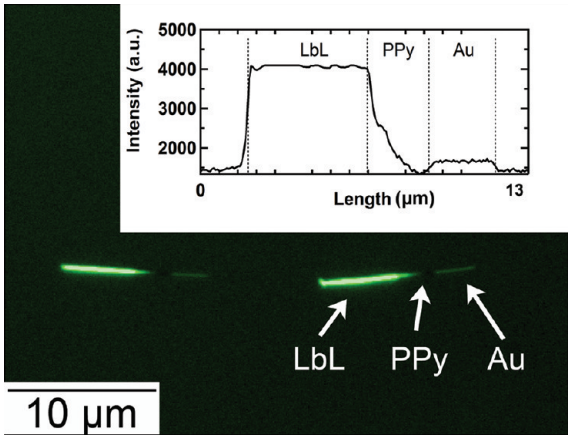

Figure 5. Fluorescent optical image of trisegmented M/PPy/LbL nanostructures composed of a gold nanowire, a PPy nanotube and a $(DNA/PAH^{FITC})_4$ LbL nanotube. Inset: Fluorescent profile traced along a trisegmented M/PPy/LbL nanostructure.

The surface treatment allowed additional nanoparticles to diffuse within the pores of the template and to electrostatically interact with the multisegmented M/PPy/LbL nanostructures. Small gold nanoparticles with a diameter of 5 nm were able to homogeneously diffuse through the LbL segments as far as within the PPy cavity (Figure 6); likewise, individual silica nanoparticles with a diameter slightly lower than the pore diameter of the template could penetrate deep in the LbL nanotubes (Figure 7a), while silica nanoparticles with a diameter close to the one of the pores were individually trapped at the end of the soft LbL segments (Figure 7b) (see the Supporting Information for complementary observations). These experiments were repeated by changing the surface charge of the nanoparticles (unmodified silica nanoparticles are negatively charged since the working pH is above the pK_a (1.7–3.5) of the silanol groups; a positive surface charge was obtained by using aminosilane-treated nanoparticles) and/or the charge of the last deposited layer (polyanion or polycation) in order to investigate the type of interactions taking place between the colloids and the multisegmented nanostructures. It was observed that neither the surface charge of the colloids nor the sign of the last deposited layer played a major role in the successful construction of such complex nanostructures. For

dx.doi.org/10.1021/cm203279z | Chem. Mater. 2012, 24, 1562–1567

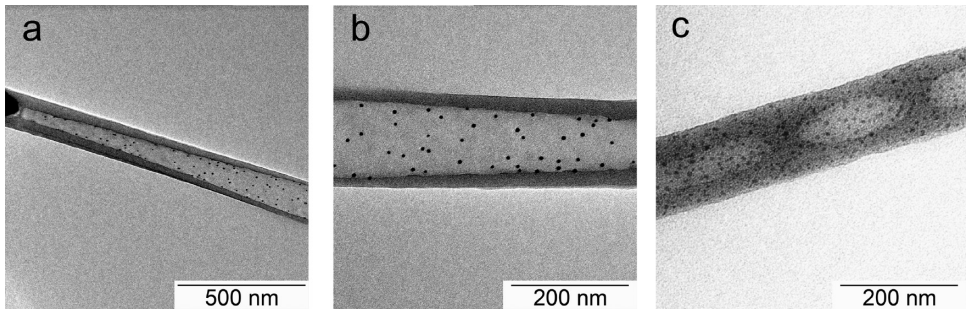

Figure 6. TEM images of the PPy and of the LbL portions of a trisegmented M/PPy/LbL nanostructure composed of a gold nanowire, a PPy nanotube, and a $(PSS/PAH)_3$ LbL nanotube exposed to a gold colloidal solution of 5 nm diameter.

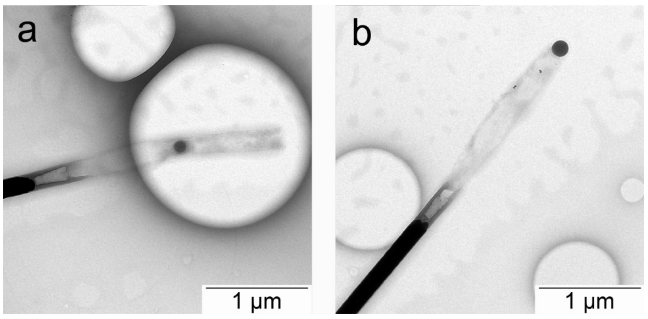

Figure 7. TEM images of trisegmented nanostructures composed of a gold nanowire, a PPy nanotube, and a $(DNA/PAE)_{4.5}$ nanotube exposed to a silica colloidal solution of 150 nm average diameter. The effectively measured silica particles diameters are (a) 130 and (b) 177 nm.

sake of redundancy, additional TEM images are displayed in the Supporting Information. The independence of the diffusion of the nanoparticles with the charge state of their surface suggests that the inner surface of the LbL nanotubes is not uniformly charged, as expected from the interpenetration of successive layers in LbL multilayer films.[41] This broadens the range of materials that can be incorporated in such colloids-functionalized multisegmented nanostructures, and demonstrates the powerful possibilities offered by the membrane-templated method to construct nanostructures of increasing complexity.

CONCLUSION

In conclusion, we have shown that the membrane-templated method can be successfully combined with different assembly techniques such as electrodeposition and layer-by-layer assembly to create various multisegmented nanostructures composed of metal, polymers, synthetic and biological polyelectrolytes, and colloids. The electrochemical approach offers control over the architectural parameters of the resulting structures (in particular the segment length and morphology), whereas the LbL adsorption technique allows nonconducting materials to be integrated within the nanostructures. The ability to easily generate such hybrid anisotropic nanoparticles with spatially resolved chemical, physical, and biochemical functionalities is very attractive for the synthesis of nanomaterials, and is highly required for electronic, sensing, and modern biomedical and biotechnological applications. For instance, these nanostructures could be useful for drug delivery applications: the PPy nanotubes – for which the dimensions and the morphology are well-defined – may serve as protecting shells for therapeutic agents incorporated inside the tubular containers through the LbL technique, while the metallic segment or the gold nanoparticles may be used for their unique optical properties allowing imaging and for photothermal therapy. Moreover, the colloidal nanoparticles capping the end of the nanostructures may be exploited to control the drug release rate in association with the biodegradability rate of the polycation PAE,[35−37] or to target the cellular uptake of the nanostructures by functionalizing the nanoparticles with specific ligands. Efforts to explore such opportunities in the elaboration of advanced drug delivery systems are currently underway in our research group.

ASSOCIATED CONTENT

Supporting Information

Some complementary results dealing with the colloidal interactions with the LbL segments are presented. This material is available free of charge via the Internet at http://pubs.acs.org

AUTHOR INFORMATION

Corresponding Author

*E-mail: sophie.demoustier@uclouvain.be.

Notes

The authors declare no competing financial interest.

ACKNOWLEDGMENTS

The authors are thankful to Dr. Etienne Ferain and *it4ip* Company for supplying polycarbonate membranes and to the Physiological Biochemistry Unit for providing access to the optical fluorescence microscope. C.J.R. is a research fellow of the F.R.S.-FNRS and S.D.-C. is a senior research associate of the F.R.S.-FNRS. Financial support was provided by the Belgian Federal Science Policy (IAP-PAI P6/27) and the F.R.S.-FNRS.

REFERENCES

(1) Skinner, K.; Dwyer, C.; Washburn, S. *Nano Lett.* **2006**, *6* (12), 2758−2762.
(2) Nicewarner-Pena, S. R.; Freeman, R. G.; Reiss, B. D.; He, L.; Pena, D. J.; Walton, I. D.; Cromer, R.; Keating, C. D.; Natan, M. J. *Science* **2001**, *294* (5540), 137−141.
(3) Kriha, O.; Zhao, L.; Pippel, E.; Gösele, U.; Wehrspohn, R. B.; Wendorff, J. H.; Steinhart, M.; Greiner, A. *Adv. Funct. Mater.* **2007**, *17* (8), 1327−1332.
(4) Bangar, M. A.; Hangarter, C. M.; Yoo, B.; Rheem, Y.; Chen, W.; Mulchandani, A.; Myung, N. V. *Electroanalysis* **2009**, *21* (1), 61−67.
(5) Kim, M. R.; Lee, D. K.; Jang, D.-J. *J. Nanomater.* **2010**, 203756.
(6) Lahav, M.; Weiss, E. A.; Xu, Q.; Whitesides, G. M. *Nano Lett.* **2006**, *6* (9), 2166−2171.

(7) Yuan, J.; Walther, A.; Muller, A. H. E. *Phys. Status Solidi B* **2010**, *247* (10), 2436−2450.
(8) Park, S.; Lim, J.-H.; Chung, S.-W.; Mirkin, C. A. *Science* **2004**, *303* (5656), 348−351.
(9) Kovtyukhova, N. I.; Martin, B. R.; Mbindyo, J. K. N.; Smith, P. A.; Razavi, B.; Mayer, T. S.; Mallouk, T. E. *J. Phys. Chem. B* **2001**, *105* (37), 8762−8769.
(10) Ren, Q.; Zhao, Y.-P.; Yue, J.; Cui, Y. *Biomed. Microdevices* **2006**, *8*, 201−208.
(11) Bauer, L. A.; Reich, D. H.; Meyer, G. J. *Langmuir* **2003**, *19* (17), 7043−7048.
(12) Son, S. J.; Bai, X.; Nan, A.; Ghandehari, H.; Lee, S. B. *J. Controlled Release* **2006**, *114* (2), 143−152.
(13) Buyukserin, F.; Medley, C. D.; Mota, M. O.; Kececi, K.; Rogers, R. R.; Tan, W.; Martin, C. R. *Nanomedicine* **2008**, *3* (3), 283−292.
(14) Son, S. J.; Lee, S. B. *J. Am. Chem. Soc.* **2006**, *128* (50), 15974−15975.
(15) Hernandez, R. M.; Richter, L.; Semancik, S; Stranick, S.; Mallouk, T. E. *Chem. Mater.* **2004**, *16* (18), 3431−3438.
(16) Callegari, V.; Demoustier-Champagne, S. *Macromol. Rapid Commun.* **2011**, *32* (1), 25−34.
(17) Martin, C. R.; Kohli, P. *Nat. Rev. Drug Discovery* **2003**, *2* (1), 29−37.
(18) Reynes, O.; Demoustier-Champagne, S. *J. Electrochem. Soc.* **2005**, *152* (9), D130−D135.
(19) Martin, C. R. *Science* **1994**, *266* (5193), 1961−1966.
(20) Martin, C. R. *Chem. Mater.* **1996**, *8* (8), 1739−1746.
(21) Park, S.; Chung, S.-W.; Mirkin, C. A. *J. Am. Chem. Soc.* **2004**, *126* (38), 11772−11773.
(22) Callegari, V.; Demoustier-Champagne, S. *ACS Appl. Mater. Interfaces* **2010**, *2* (5), 1369−1376.
(23) Cao, G.; Liu, D. *Adv. Colloid Interface Sci.* **2008**, *136* (1−2), 45−64.
(24) Decher, G. *Science* **1997**, *277*, 1232−1237.
(25) Alem, H.; Blondeau, F.; Glinel, K.; Demoustier-Champagne, S.; Jonas, A. M. *Macromolecules* **2007**, *40* (9), 3366−3372.
(26) Cuenot, S.; Alem, H.; Louarn, G.; Demoustier-Champagne, S.; Jonas, A. M. *Eur. Phys. J. E* **2008**, *25*, 343−348.
(27) Ariga, K.; Hill, J. P.; Ji, Q. *Phys. Chem. Chem. Phys.* **2007**, *9* (10), 2319−2340.
(28) Wang, Y.; Angelatos, A. S.; Caruso, F. *Chem. Mater.* **2008**, *20* (3), 848−858.
(29) Liang, Z.; Susha, A. S.; Yu, A.; Caruso, F. *Adv. Mater.* **2003**, *15* (21), 1849−1853.
(30) Ai, S.; Lu, G.; He, Q.; Li, J. *J. Am. Chem. Soc.* **2003**, *125* (37), 11140−11141.
(31) Kim, D. H.; Karan, P.; Göring, P.; Leclaire, J.; Caminade, A.-M.; Majoral, J.-P.; Gösele, U.; Steinhart, M.; Knoll, W. *Small* **2005**, *1* (1), 99−102.
(32) Qu, X.; Lu, G.; Tsuchida, E.; Komatsu, T. *Chem.—Eur. J.* **2008**, *14* (33), 10303−10308.
(33) Landoulsi, J.; Roy, C. J.; Dupont-Gillain, C.; Demoustier-Champagne, S. *Biomacromolecules* **2009**, *10* (5), 1021−1024.
(34) Komatsu, T.; Qu, X.; Ihara, H.; Fujihara, M.; Azuma, H.; Ikeda, H. *J. Am. Chem. Soc.* **2011**, *133* (10), 3246−3248.
(35) Lynn, D. M.; Langer, R. *J. Am. Chem. Soc.* **2000**, *122* (44), 10761−10768.
(36) Zhang, J.; Fredin, N. J.; Janz, J. F.; Sun, B.; Lynn, D. M. *Langmuir* **2006**, *22* (1), 239−245.
(37) Zhang, J.; Fredin, N. J.; Lynn, D. M. *J. Pol. Sci., Part A: Polymer Chemistry* **2006**, *44* (17), 5161−5173.
(38) Roy, C. J.; Dupont-Gillain, C.; Demoustier-Champagne, S.; Jonas, A. M.; Landoulsi, J. *Langmuir* **2010**, *26* (5), 3350−3355.
(39) Roy, C. J.; Leprince, L.; De Boulard, A.; Landoulsi, J.; Callegari, V.; Jonas, A. M.; Demoustier-Champagne, S. *Electrochim. Acta* **2011**, *56* (10), 3641−3648.
(40) Callegari, V.; Gence, L.; Faniel, S.; Gustin, C.; Melinte, S.; Bayot, V.; Reynes, O.; Demoustier-Champagne, S. *Phys. Rev. B* **2007**, *76*, 115415.
(41) Liu, G.; Zhao, J.; Sun, Q.; Zhang, G. *J. Phys. Chem. B* **2008**, *112* (11), 3333−3338.